



Development of micro-hotplate and its reliability for gas sensing applications

Mahanth Prasad^{1,2} · Partha S. Dutta²

Received: 3 August 2018 / Accepted: 19 October 2018 / Published online: 30 October 2018
© Springer-Verlag GmbH Germany, part of Springer Nature 2018

Abstract

This paper presents the development of a double spiral micro-heater and its reliability testing for gas sensing applications. The design and simulation of the micro-hotplate was carried out using MEMS-CAD Tool COVENTORWARE. The micro-hotplate structure consists of a 1.0 μm -thick thermally grown SiO_2 membrane of area $600 \mu\text{m} \times 600 \mu\text{m}$ over which a double spiral platinum resistor has been fabricated. A platinum resistor of 117Ω is fabricated on SiO_2 layer using lift-off technique. The platinum deposition was carried out using DC sputtering technique. The hotplate membrane release was accomplished by using both wet and dry etching of silicon. The temperature coefficient of resistance (TCR) of platinum as measured was found to be $2.19 \times 10^{-3}/^\circ\text{C}$. This value has been used to estimate the micro-hotplate temperature. The micro-hotplate consumes only 50 mW power when heated up to 500°C . The results of reliability testing of fabricated device using pulse mode of operation, maximum current capability and thermal stability have been presented. The hotplate has been shown to continuously operate at 500°C for more than 4 h and sustain maximum current of 23 mA and 130 cycles of pulse mode operation without any damage to the structure.

1 Introduction

Solid-state gas sensor was reported more than 5 decades ago [37]. Since then, rapid progress has been made ranging from Taguchii type sensors to sophisticated low-power micro electro mechanical systems (MEMS)-based CMOS compatible sensors for large-scale integration within various gas sensing systems [1, 8, 16, 17, 34, 35, 40, 44]. Based on extensive experimental and theoretical research, the key parameters of gas sensors such as selectivity, sensitivity, and response time have been improved by integrating them with thermally controlled MEMS device platforms [27]. These devices are categorized as micro-hotplates. The micro-hotplates are required to provide high operating temperatures in the range of $250\text{--}500^\circ\text{C}$ that are needed for

metal oxide-based thin film sensors [18]. Commonly used metal-oxides for gas sensing applications are SnO_2 , Fe_2O_3 and ZnO . Among these gas sensing films, SnO_2 is commonly used because of its quick response time [21]. The sensing activity is due to the redox reaction between target gas and the sensing layer at a specific temperature.

Various technologies such as silicon [1, 43], silicon on insulator, SOI [2, 14], porous silicon [24], screen printing [36], ceramics [20] flexible substrate [29], LTCC [22] and laser micromachining [28], have been used to develop the micro-hotplate platform. Each technology has its own advantages and disadvantages based on its power consumption, response time, chip size, cost, flexibility and reliability. In SOI technology, Friedberger A et al. reported the ultra-low dc power consumption (12 mW at 600°C), fast transient time, good thermal stability and high reproducibility. However, the use of commercial SOI-CMOS process followed by a deep reactive ion etching (DRIE) increases the cost of device. Amongst the above technologies, silicon has the advantages of small size, low power consumption and compatibility with CMOS processing.

The electrical and mechanical stability of heater structure used for gas sensing is important because of their thermal expansion effects, compatibility with CMOS processing and stress constraints over the membrane [40, 46].

✉ Mahanth Prasad
mahanth.prasad@gmail.com

Partha S. Dutta
duttap@rpi.edu

¹ Transducers and Actuators Group, CSIR-Central Electronics Engineering Research Institute (CEERI), Pilani, Rajasthan 333031, India

² Electrical, Computer and Systems Engineering Department, Rensselaer Polytechnic Institute, Troy, NY 12180, USA

The reliability of micro-hotplate mainly depends on (i) selection of heating and membrane materials, (ii) heater geometry, (iii) type of membrane (close or open) and (iv) the fabrication technique. Different heating materials such as NiFe [12], SiC–N [7], polysilicon [1], molybdenum [25], DilverP1 [8], platinum [31, 32] and Tungsten [2] have been used by different researchers. Suitable heating material should have the properties of (i) high thermal conductivity, (ii) low thermal expansion coefficient, (iii) high melting point, (iv) low Poisson's ratio, large young's modulus and (v) compatibility with standard silicon fabrication technology. The heating material, polysilicon, is most widely used for microheater because of its compatibility with CMOS processing. However, the resistivity of polysilicon is unstable at 550 °C due to its grain instability. The use of Ni as a heater has the disadvantage of low resistivity. The Ni alloy (mixture of Fe, Ni and Co) known as Dilver P1 has high resistivity, high yield stress and low thermal expansion coefficient. The microheater based on Dilver P1 provides good strength in comparison to other heating materials. However, more research is required to study the fabrication and reliability of this material. Molybdenum is also used as a heating material. It is shown to perform better than platinum in terms of maximum operating temperature and stability of resistance [25]. However, it oxidizes at lower temperature and, therefore, passivation of this material is required to operate at higher temperatures. Among the above heating materials, platinum is an ideal candidate for micro-hotplate applications. It has stable temperature coefficient of resistance (TCR), high melting point, high reliability, reproducibility, good thermal conductivity and moderate coefficient of thermal expansion. Also, Platinum can handle large current densities and operate up to 550–600 °C without any structural damage [41].

The membrane materials play an important role to provide a platform for microheaters, electrodes and sensing layer. In most of the cases, the membrane is made of either silicon dioxide [1, 31, 32] or silicon nitride [11, 15] or a combination of both (oxinitride) [3–6, 13, 19, 23, 26]. In recent years, new materials such as SiC [38] and polyimide [10] have also been proposed. But SiC-based micro-hotplate has complex process technology. Rossi et al. [33], reported the compressive stress of dielectric silicon dioxide and tensile stress of dielectric silicon nitride layer. The stacked thin layer of silicon dioxide and silicon nitride improves the mechanical properties of hotplate membrane as well as fabrication yield of device. However, silicon nitride layer has variation and uncertainty in thermal conductivity (1.0–30 W/m K at 300 K) [8], which may vary the temperature uniformity and thermal isolation of heater.

In order to reduce the power consumption and improve the temperature uniformity, different geometries of microheaters have been studied [1, 8, 30, 39, 42]. The key

fabrication technique for different types of membranes for gas sensors is based on micromachining of silicon. Hotplate membrane can be classified in two categories: (i) bridge membrane type structure [8, 31, 45] and (ii) full membrane type structure. The bridge type membrane structure becomes more fragile and reduces the reliability of devices. Also, the deposition and patterning of sensing film becomes complex after the release of hotplate membrane. However, in case of close type or full membrane type structure, the researchers used DRIE technique to release the structure. The use of DRIE to release the structure is an expensive process and increases the cost of devices.

This paper presents a new approach for overcoming the reliability issues and reducing the fabrication cost of micro-hotplates by reducing the process complexity for sensing film deposition and patterning. This technique also makes the structure less fragile and improves the wafer handling during device fabrication. In order to reduce the number of process steps and variation in thermal conductivity of the hotplate membrane, only a single dielectric SiO₂ layer has been used for the microhotplate membrane. Platinum has been selected as the heating material in the present study. The use of double spiral shaped Pt-heater provides better temperature uniformity. Stable TCR of heating material is required for reliable operation of the device. In the sections below, we elaborate on the structural design, fabrication process, characterization of the devices and their reliability testing.

2 Structural design

The complete gas sensor based on microhotplate is shown in Fig. 1. The structure consists of the following: (i) thermally insulated dielectric suspended membrane made on silicon substrate using bulk micromachining, (ii) heating element fabricated on the membrane, (iii) thin insulating layer to avoid the contact between heating element and interdigitated fingers, (iv) interdigitated fingers to reduce the resistivity of

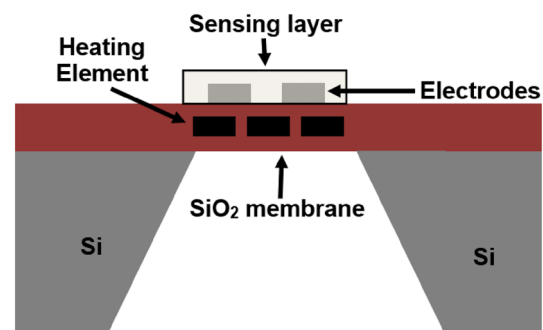


Fig. 1 Schematic of microhotplate-based gas sensor

the sensing film and (v) sensing layer for gas sensing. The heat transfer analysis has been carried out for this structure. Heat transfer from different locations of the microhotplate membrane occurs due to a combination of conduction, convection and radiation. Along the hotplate membrane, heat conduction dominates. However, above and below the membrane heat transfer occurs due to all three factors. The heat loss through or from the hotplate membrane can be expressed as [40],

$$Q_{\text{tot}} = G_m \lambda_m (T_{\text{hot}} - T_{\text{amb}}) + G_{\text{air}} \lambda_{\text{air}} (T_{\text{hot}} - T_{\text{amb}}) + G_{\text{rad}} \epsilon \sigma (T_{\text{hot}}^4 - T_{\text{amb}}^4) + \Delta x, \quad (1)$$

where, the first term on the right-hand side of the equation is due to heat conduction through the membrane, second term is due to heat conduction through the ambient air, the third term is heat loss due to radiation and the last term accounts for unknown heat losses including free convection. In this expression, G_m , G_{air} and G_{rad} are geometric factors related to the specific membrane architecture, T_{hot} and T_{amb} denote the temperature of the hot active area and the ambient, respectively. The λ_m and λ_{air} are thermal conductivity of the membrane and the surrounding atmosphere, ϵ , is the emissivity of the membrane material and σ is the Stefan–Boltzmann constant.

For suspended type membrane, heat conduction along four suspension beams with length l and cross-sectional area A_{beam} is given as follows:

$$Q_{\text{beam}} = \frac{4(\lambda_{\text{beam}} A_{\text{beam}})(T_{\text{hot}} - T_{\text{amb}})}{l}, \quad (2)$$

whereas λ_{beam} is the thermal conductivity of the beam,

$$G_{\text{mem}} = \frac{4A_{\text{beam}}}{l}. \quad (3)$$

For closed membranes, the square membrane can be replaced by a round one and the heat conduction is given by

$$Q_{\text{mem}} = \frac{2\pi \lambda_m d (T_{\text{hot}} - T_{\text{amb}})}{\ln(r_a/r_i)} \quad (4)$$

$$G_{\text{mem}} = \frac{2\pi d}{\ln(r_a/r_i)}, \quad (5)$$

where d denotes the thickness of the membrane, r_i and r_a

are the radii of the heated area and the membrane area, respectively.

As evident from Eqs. (2) and (4), it is desirable to choose the membrane of lower conductivity and smaller thickness to achieve low thermal losses. In general, the total power consumption can be minimized by constructing thin membranes having low thermal conductivity, adjusting the heater size, decreasing the heated area and choosing a large pit depth. In the present work, closed type membrane has been studied. The dimensions of structure are as follows: membrane size: $600 \mu\text{m} \times 600 \mu\text{m}$, thickness of membrane: $1.0 \mu\text{m}$, thickness of heater: $0.2 \mu\text{m}$, heater finger width: $20 \mu\text{m}$ and space between fingers: $20 \mu\text{m}$. The structure was designed and simulated using MEMS-CAD Tool COVENTORWARE. The results are shown in Fig. 2. The temperature distribution plot at an applied voltage of 5 V is shown in Fig. 2a. The variation in temperature from the center to the edge of the membrane is expected due to the higher temperature at the central area of the membrane. At 5 V, the average maximum temperature, maximum displacement (in z axis) and von mises stress of the hotplate were found to be $921.7 \text{ }^\circ\text{C}$ (Fig. 2a), $0.1 \mu\text{m}$ (Fig. 2b) and 1987 MPa (Fig. 2c), respectively. The stacked thin layer of silicon dioxide and silicon nitride can overcome the stress problem of hotplate membrane [33].

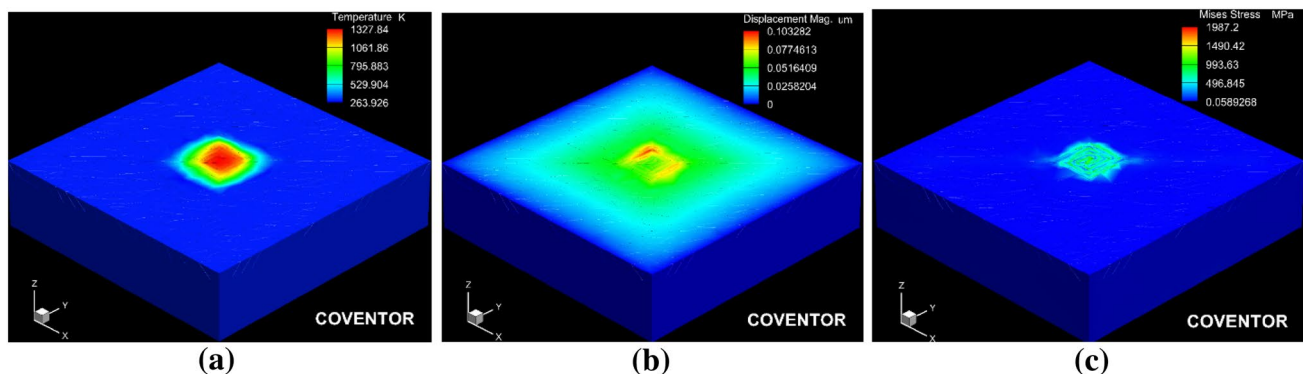


Fig. 2 Simulation of double spiral microhotplate using MEMS tool COVENTORWARE: **a** temperature distribution at 5 V, **b** displacement at 5 V, **c** von mises stress distribution at 5 V

But this also increases the number of process steps during device fabrication. Fig. 2a shows good temperature uniformity in the active area of the hotplate membrane. However, the bending portion of heater shows moderate to high stress accumulation.

3 Fabrication processes

The fabrication process of the device is dictated by the substrate and heating materials. The reliability of the device depends on both the substrate and the heater design. Two primary goals for any design are low power consumption and uniform temperature across active area. Because of fragile structures, microhotplate with high mechanical strength is needed for all processing steps. Therefore, micromachined substrate should be stable during deposition of the sensing film and subsequent processing. This section presents the fabrication technique of a microhotplate on silicon substrate used for gas sensing applications. A process flow for fabrication of microhotplate using closed type membranes is shown in Fig. 3. The basic fabrication process steps are presented below:

3.1 Substrate cleaning

The first step in the fabrication process starts with selection of p-type silicon wafers of orientation $\langle 100 \rangle$ and resistivity, 10–20 Ω cm. The silicon wafers were cleaned using piranha solution. The solution was prepared using sulfuric acid (concentration 98%) and H_2O_2 (concentration 30%) in the volume ratio of 3:1. The wafers were finally rinsed in deionized (DI) water and dried with nitrogen.

3.2 Oxidation

The freshly cleaned wafers were used for thermal oxidation in an oxidation furnace at 1050 $^\circ\text{C}$. The grown silicon dioxide layer acts as a masking layer during silicon micromachining. This layer also acts as a platform for microheater.

3.3 Heater fabrication

The platinum heater is fabricated using lift-off technique (Fig. 4a). In this case, platinum layer is deposited using DC magnetron sputtering system on a patterned wafer with positive photoresist. An adhesive Ti layer of 20 nm thickness is deposited before platinum. Typical sputtering process parameters such as base pressure, deposition pressure, power and deposition temperature are: 3.99×10^{-7} mbar; 6.66 mbar; 200 W and 50 $^\circ\text{C}$, respectively. Finally, platinum lift-off is carried out using acetone to remove the platinum from unwanted area. After the lift-off process, the wafer is

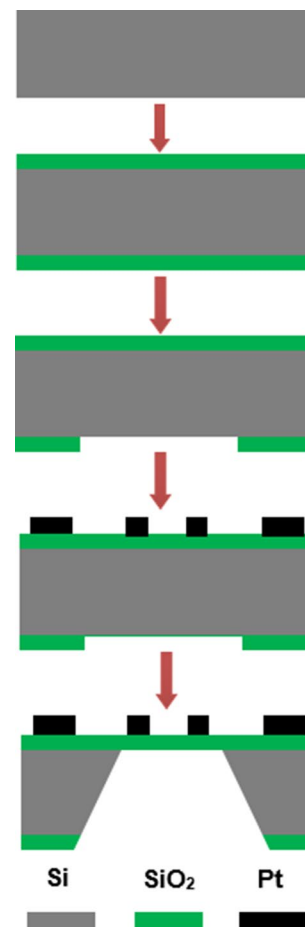


Fig. 3 Process flow diagram for fabrication of microhotplate

exposed to a O_2 plasma to remove any photoresist residues. In case of complete gas sensor fabrication, heater passivation is required before the interdigitated fingers and sensing layer deposition. The interdigitated fingers are used to measure the resistance of sensing film during gas exposure. The passivation process is used to isolate the heater from the interdigitated fingers and also protect it from any chemicals attack during membrane formation.

3.4 Membrane release

This is the last process step for either a hotplate fabrication or a complete gas sensor fabrication. The membrane release is carried out using micromachining techniques. Bulk micromachining is used to make microstructures, trenches and holes in the substrate. This is implemented using selective etching of silicon in order to create the structures on the device. Wet and dry etchings of silicon are commonly used for this purpose. In case of dry etching, deep reactive ion etching (DRIE) technique is being used. In case of wet etching of silicon, three different

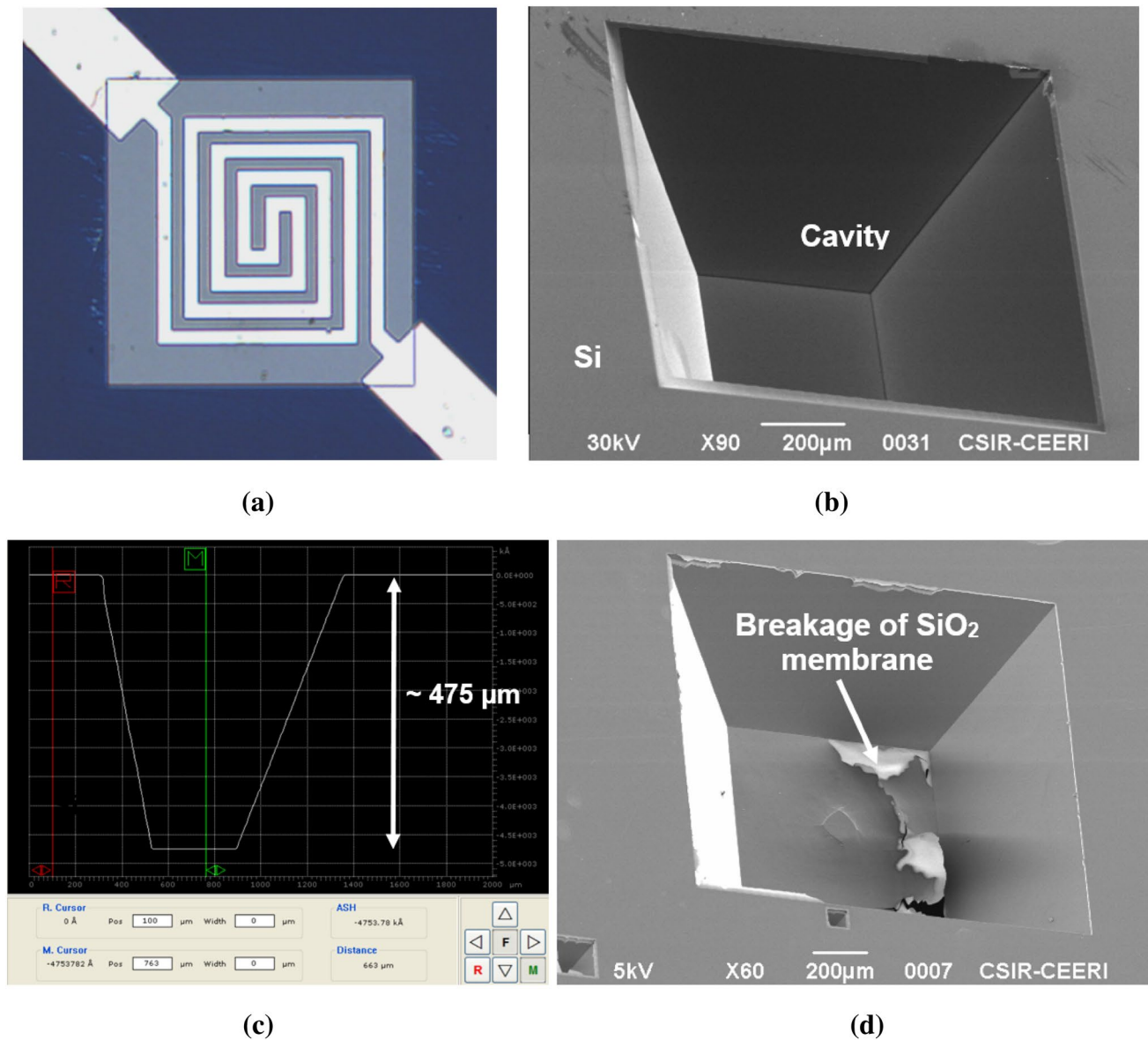


Fig. 4 Fabrication of double spiral microhotplate: **a** Pt-heater fabricated on SiO_2 layer, **b** SEM image of micromachined structure from backside etched up to $475\ \mu\text{m}$ depth, **c** cavity depth measured using

Dektak 6M surface profiler and **d** SEM image of SiO_2 membrane breakage after complete removal of Si using TMAH solution

etchants, namely potassium hydroxide (KOH), tetra-methyl ammonium hydroxide (TMAH) and ethylene di-amine pyro-catechol (EDP) have been used. KOH is a nontoxic, economical and commonly used alkali metal hydroxide silicon etchant. However, it produces potassium ions on wafer surface during micromachining. Also, it is highly corrosive and attacks aluminum that makes it undesirable for CMOS fabrication. EDP is a diamine-based etchant which has high Si/ SiO_2 etch rate ratio, low degree of anisotropy, partly CMOS compatible and toxic in comparison to KOH and TMAH. The TMAH is most suitable for silicon etching and was used for bulk micromachining

in the present studies. The complete removal of silicon, approximately up to a wafer thickness is required for hot-plate membrane formation. DRIE technique is most suitable for bulk micromachining of silicon because it has controlled etch rate as compared to wet etching technique. However it is costly and it is necessary to run the process for long duration of time to release the hotplate membrane. In addition, a thick SiO_2 layer or an extra metal layer (Al) is required to remove the silicon. In the present approach, membrane was released in two steps: (i) First of all, a deep cavity of $475\ \mu\text{m}$ was etched by TMAH solution (Fig. 4b). The process was carried out in 25% wt.

TMAH solution at 85 °C temperature. For uniform bulk micromachining of silicon, the wafer holder was rotated with a speed of 5 rpm. The cavity depth was measured using Dektak 6M surface profiler as shown in Fig. 4c. The sensing film deposition and patterning can be done after this step due to sufficient strength of the diaphragm. (ii) The remaining 25 µm thickness of silicon below the membrane was removed using DRIE technique. The use of both techniques, first wet (TMAH) and then dry (DRIE) for hotplate membrane formation, reduces the fabrication cost and process complexity of sensing film deposition. This approach also avoids the attack of TMAH solution on sensing film during bulk micromachining. The yield of the process using the wet (TMAH) and dry (DRIE) approach has been found to increase to 80%. For comparison, the yield of the process in case of only wet etching technique is around 20%. This is because of silicon removal makes the wafer more fragile. This leads to more damages, particularly in membrane areas during etching, cleaning, rinsing and drying processes. Figure 4d shows one of the breakage SiO₂ membrane after complete removal of Si using wet etching technique.

4 Characterization

Characterization of microheaters mainly involves the measurement of hotplate membrane temperature. In electrical characterization, the resistance dependence on voltage was analyzed. By measuring I – V characteristics of microheater, device parameters such as breakdown voltage, maximum temperature of device operation, power consumption, mechanical strength and reliability can be estimated. Testing processes and results of the developed double spiral platinum-based microhotplate are presented below:

4.1 Temperature coefficient of resistance (TCR)

The temperature coefficient of resistance (TCR) of the platinum heater is an important parameter and can be measured by electrically heating the device in a temperature-controlled oven. By using TCR value, the temperature of platinum heater can be obtained by the following equation:

$$T_2 = T_1 + \frac{R_2 - R_1}{R_1 \times \text{TCR}}, \quad (6)$$

where R_1 and R_2 are the heater resistances at temperatures T_1 and T_2 , respectively [1]. This method gives the approximate

value of membrane temperature instead of exact temperature. However, it is a convenient way to estimate the temperature. Using this technique, the TCR value of platinum heater was measured to be 0.0021/°C.

4.2 Power consumption

In order to measure the membrane temperature, diced microhotplate chip was used. The experimental set-up MPS 150 probe station is shown in Fig. 5a. The voltage is varied across the microheater. The power consumption versus temperature plot of the microhotplate as recorded is shown in Fig. 5b. The I – V characteristic is shown in Fig. 5c. Test results show that the microhotplate consumes 50 mW power when heated up to 500 °C.

4.3 Transient response time

This is defined as the time taken to heat the device to obtain the maximum uniform temperature across the active area. In order to have the low power consumption of hotplate, the response time should be minimum. In pulse mode of operation of hotplate, the heat pulse may be correspondingly reduced resulting in lower duty cycle and, therefore, lower power consumption. The transient response can be obtained by using I – V measurement with change in bias voltage. In the present studies, the response time of the heater was found to be less than 1 ms.

5 Reliability studies

Reliability of microhotplates depends on the thermal and mechanical behavior of the devices. The simulation models of microhotplates and its accelerated aging test protocols were developed to investigate the failure mechanisms. The maximum reachable temperature of microhotplate and its stability influence the reliability of the device. Amongst various heating materials, platinum-based microheaters are more robust than those made of polysilicon, molybdenum and DilverP1. The reliability of the developed device was evaluated using the following parameters:

5.1 Current carrying capability

For safe operation of microhotplate, the current carrying capability of microheater must be evaluated. This parameter can be obtained using the experimental data shown in Fig. 5c depicting that the maximum current of 23.3 mA can pass through the heater without any damage. Once the structure becomes damaged (Fig. 5d), the measured resistance across the microheater increases to a very high value in the giga-ohm range.

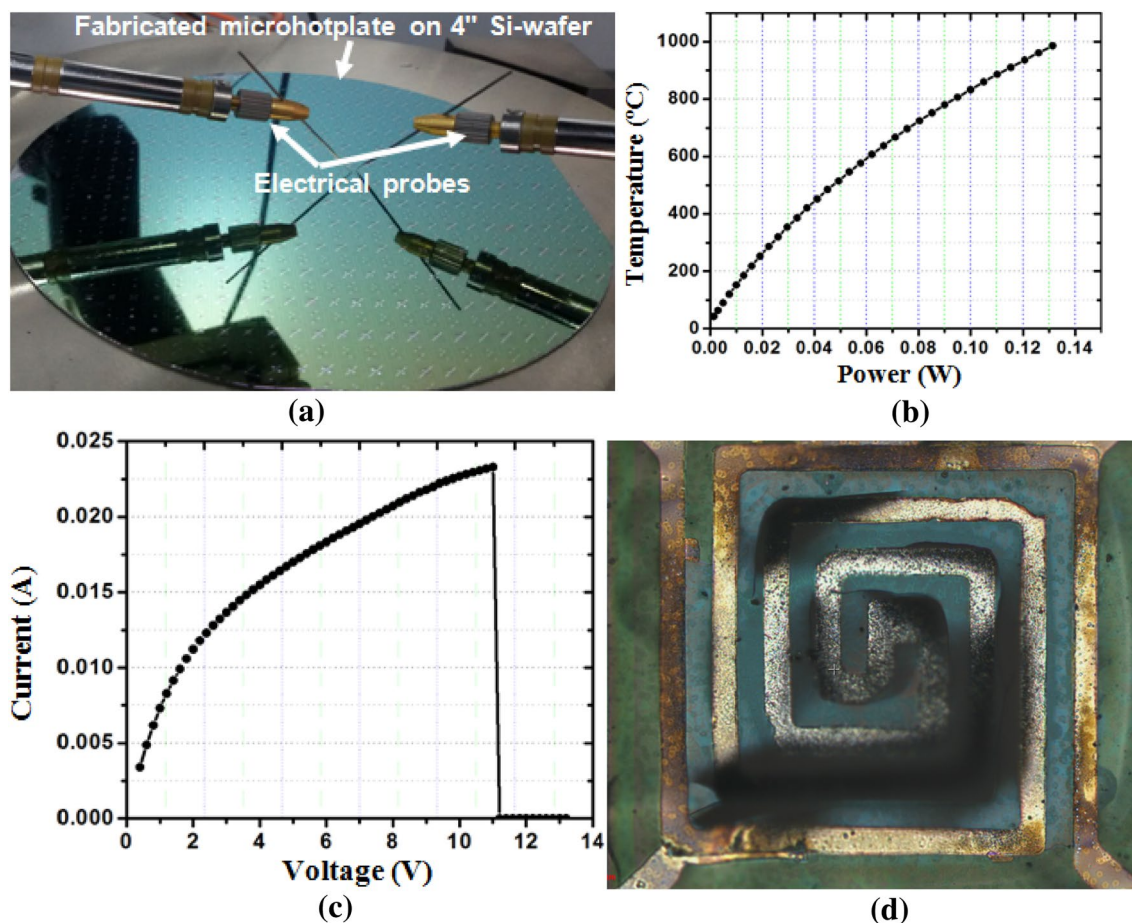


Fig. 5 Characterization of microheater: **a** testing set up, **b** power consumption versus temperature and **c** I - V characteristics and **d** optical image of burned heater after passing maximum current

5.2 Pulse-mode operation

The pulse-mode of operation of microhotplate is widely used in gas sensor. This mode of operation requires minimum temperature drift due to frequent mechanical deformation associated with the on-off cycles. In this mode of operation, microhotplate produces an elevated temperature in the active area of the membrane for a certain time duration. For gas sensing, normal pulse-mode operation time is 5 s at 400 °C and 10 s at 100 °C [9]. Pulse-mode operation of fabricated microhotplate structure is shown in Fig. 6. Here, a pulse of 10 s ($t_{\text{on}} = 5 \text{ s} + t_{\text{off}} = 5 \text{ s}$) is applied to the microheater. The resistance variation of heater at different applied voltages 5 V, 6 V, 7 V and 8 V is shown in Fig. 6a. The corresponding temperatures at different applied voltages 5 V, 6 V, 7 V and 8 V are found to be 715 °C, 856 °C, 972 °C and 1083 °C, respectively (Fig. 6b). The results showed that the microhotplate structure can sustain at least 130 cycles of pulse mode operation at different values of applied voltages, (5 V, 6 V and 7 V) without any damage to the structure. However, at

$V_{\text{max}} = 8 \text{ V}$, the structure sustained only 50 cycles of pulse mode operation prior to failure. The general trend shows that increasing the operating temperature of microhotplate leads to decrease in the reliability of the microhotplate in the pulse mode operation.

5.3 Thermal stability

This parameter can be tested by applying a constant voltage across the heater. In order to determine the thermal stability, the first step is to calculate the temperature of membrane using Eq. (6). Thermal stability of structure is tested by applying a constant voltage across double spiral heater for long time duration. As shown in Fig. 7, at an applied voltage, $V = 3.5 \text{ V}$ for 4.1 h, the resistance value of microheater is found to be $239 \pm 0.5 \Omega$. At $V = 5.5 \text{ V}$, the resistance value of microheater for same time duration was found to be $310 \pm 1.5 \Omega$. Hence, it can be seen that if applied voltage across heater is increased, the deviation in resistance or temperature of microhotplate is also increased. In case of $V = 7.5 \text{ V}$ and 8.5 V , resistance of microheater becomes

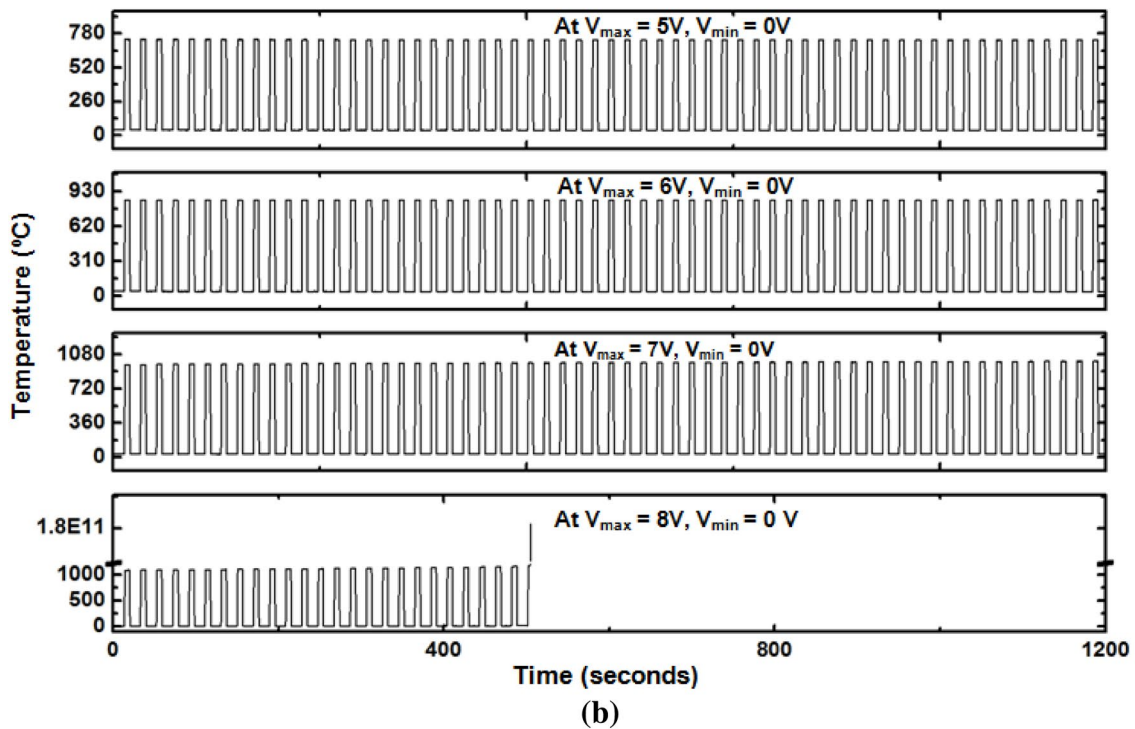
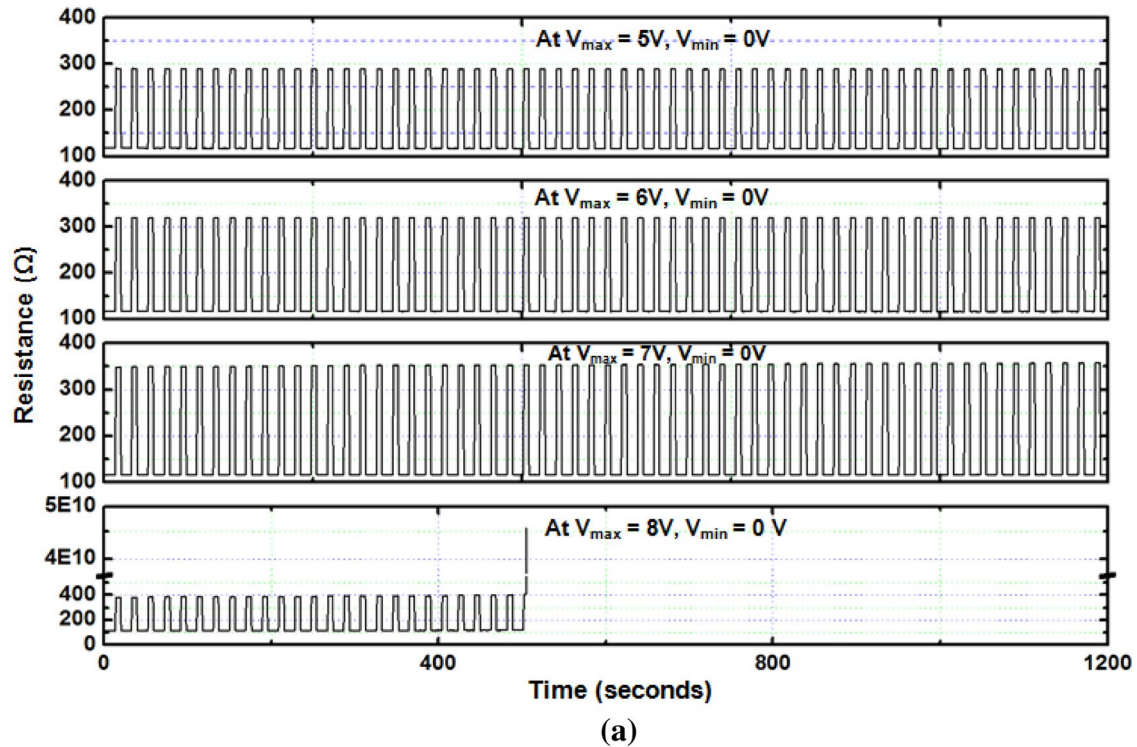


Fig. 6 Experimental results of resistance dependence (thermal stability) of microheater versus testing time at different applied voltages

very high after certain time and performance of the device is significantly degraded. Thus the operation time limit of microhotplate decreases as applied voltage is increased.

6 Conclusion

The microhotplate technology has been presented highlighting the key elements such as heating materials and

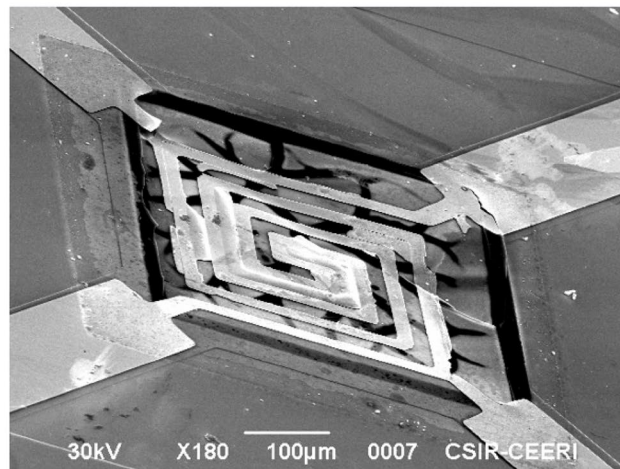
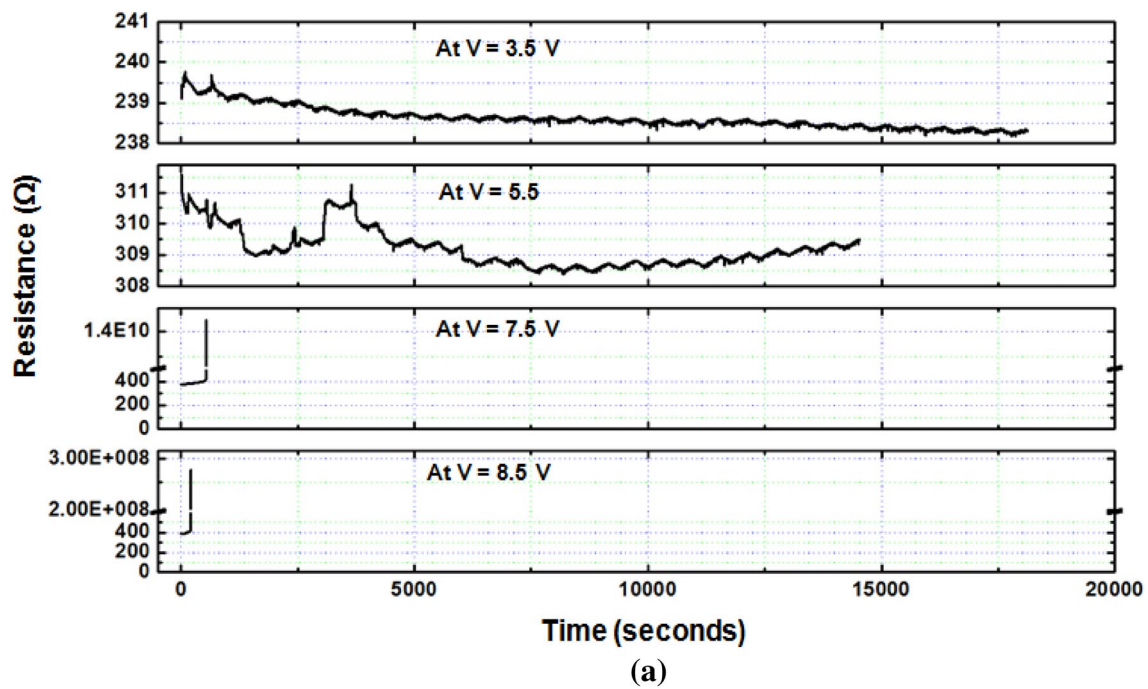


Fig. 7 Thermal stability testing: **a** microheater resistance versus testing time at different applied voltages, **b** optical image of heater glow before breakage and **c** SEM image of damaged structure

membrane materials for heaters. A double spiral Pt-based microhotplate has been designed, fabricated and tested. Sequential wet and dry bulk micromachining of silicon has been found to improve the yield of devices. This process makes the structure less fragile and improves the wafer handling capability. Also, it reduces the fabrication cost and process complexity of sensing film deposition during fabrication of device. The yield of the process using this technique is found to be 80%. The TCR value of platinum was measured to estimate the hotplate temperature. The device was characterized with respect to various

reliability parameters such as power consumption, current carrying capability, pulse mode of operation and thermal stability. The microhotplate consumes only 50 mW when heated up to 500 °C. Also, the hotplate can sustain a maximum current of 23.3 mA and 130 cycles of pulse mode operation at different values of applied voltages, (5 V, 6 V and 7 V) without any damage.

Acknowledgements The authors wish to thank the Director, CSIR-CEERI, Pilani for encouragement and guidance. They are also thankful to all members of Smart Sensor Area for helpful discussions, technical assistance and support.

References

- M.Y. Afridi, J.S. Suehle, M.E. Zaghoul, D.W. Berning, A.R. Hefner, R.E. Cavicchi, C.J. Taylor, A monolithic CMOS micro-hotplate based gas sensor system. *IEEE Sens. J* **2**(6), 644–655 (2002)
- S.Z. Ali, F. Udrea, W.I. Milne, J.W. Gardner, Tungsten-based SOI microhotplates for smart gas sensors. *J. Microelectromech. Syst.* **17**(6), 1408–1417 (2008)
- S. Astié, A.M. Gué, E. Scheid, J.P. Guillemet, Design of low power SnO₂ gas sensor integrated on silicon oxynitride membrane. *Sens. Actuators B* **67**, 84–88 (2000)
- E. Barborini, S. Vinati, M. Leccardi, P. Repetto, G. Bertolini, O. Rorato, L. Lorenzelli, M. Decarli, V. Guarnieri, C. Ducati, P. Milani, Batch fabrication of metal oxide sensors on micro-hotplates. *J. Micromech. Microeng.* **18**(5), 1–7 (2008)
- M. Baroncini, P. Placidi, G.C. Cardinali, A. Scorzoni, Thermal characterization of a microheater for micromachined gas sensors. *Sens. Actuators A Phys.* **115**(1), 8–14 (2004)
- J.C. Belmonte, J. Puigcorbe, J. Arbiol, A. Vila, J.R. Morante, N. Sabate, I. Gracia, C. Cane, High-temperature low-power performing micromachined suspended micro-hotplate for gas sensing applications. *Sens. Actuators B Chem.* **114**(2), 826–835 (2006)
- G. Benn, Design of a silicon carbide micro-hotplate geometry for high temperature chemical sensing. M.S. thesis, MIT, Cambridge, 2001
- P. Bhattacharyya, Technological journey towards reliable micro-heater development for MEMS gas sensors: a review. *IEEE Trans. Device Mater. Reliab.* **14**(2), 589–599 (2014)
- J.M. Bosc, Y. Guo, V. Sarihan, T. Lee, Accelerated life testing for micro-chemical sensors. *IEEE Trans. Reliab.* **47**(2), 135–141 (1998)
- D. Briand, S. Colin, J. Courbat, S. Raible, J. Kappler, N.F. de Rooij, Integration of MOX gas sensors on polyimide hotplates. *Sens. Actuators B Chem.* **130**(1), 430–435 (2008)
- D. Briand, S. Heimgartner, M. Gretillat, B. Schoot, N.F. Rooij, Thermal optimization of microhotplates that have a silicon island. *J. Micromech. Microeng.* **12**(6), 971–978 (2002)
- U. Dibbern, A substrate for thin-film gas sensors in microelectronic technology. *Sens. Actuators B Chem.* **2**(1), 63–70 (1990)
- I. Elmi, S. Zampolli, E. Cozzani, M. Passini, G.C. Cardinali, M. Severi, Development of ultra low power consumption hotplates for gas sensing applications, in *Proc. IEEE Sensors*, pp. 243–246 (2006)
- A. Friedberger, P. Kreisl, E. Rose, G. Muller, G. Kuhner, J. Wollenstein, H. Bottner, Micromechanical fabrication of robust low-power metal oxide gas sensors. *Sens. Actuators B* **93**, 345–349 (2003)
- P. Fujres, C. Ducso, M. Adam, J. Zettner, I. Barsony, Thermal characterization of micro-hotplates used in sensor structures. *Superlattices Microstruct.* **35**(3–6), 455–464 (2004)
- K.G. Girija, S. Chakraborty, M. Menaka, R.K. Vatsa, A. Topkar, Low-cost surface micromachined microhotplates for chemiresistive gas sensors. *Microsyst. Technol.* **24**(8), 3291 (2018) (p 7)
- M. Graf, D. Barrettino, H.P. Baltes, A. Hierlemann, CMOS Hotplate Chemical Microsensors (Springer, Berlin, 2007)
- M. Graf, D. Barrettino, K.U. Kirstein, A. Hierlemann, CMOS microhotplate sensor system for operating temperatures up to 500 °C. *Sens. Actuators B* **117**, 346–352 (2006)
- B. Guo, A. Bermak, P.C.H. Chan, G. Yan, An integrated surface micromachined convex microhotplate structure for tin oxide gas sensor array. *IEEE Sens. J* **7**(12), 1720–1726 (2007)
- E.E. Karpov, E.F. Karpov, A. Suchkov, S. Mironov, A. Baranov, V. Sleptsov, L. Calliari, Energy efficient planar catalytic sensor for methane measurement. *Sens. Actuators A Phys.* **194**, 176–180 (2013)
- H.J. Kim, J.H. Lee, Highly sensitive and selective gas sensors using p-type oxide semiconductors: overview. *Sens. Actuators B* **192**(1), 607–627 (2013)
- L. Kulhari, P.K. Khanna, Design, simulation and fabrication of LTCC-based microhotplate for gas sensor applications. *Microsyst. Technol.* **24**, 2169–2175 (2018)
- D.S. Lee, S.W. Ban, M. Lee, D.D. Lee, Micro gas sensor array with neural network for recognizing combustible leakage gases. *IEEE Sens. J.* **5**(3), 530–536 (2005)
- P. Maccagnani, R. Angelucci, P. Pozzi, A. Poggi, L. Dori, G.C. Cardinali, P. Negrini, Thick oxidised porous silicon layer as a thermoinsulating membrane for high-temperature operating thin- and thick-film gas sensors. *Sens. Actuators B* **49**, 22–29 (1998)
- L. Mele, F. Santagata, E. Iervolino, M. Mihailovic, T. Rossi, A.T. Tran, H. Schellevis, J.F. Creemer, P.M. Sarro (2012), A molybdenum MEMS microhotplate for high temperature operation, *Sens. Actuators A* **188**, 173–180
- Y. Mo, Y. Okawa, K. Inoue, K. Natukawa, Low-voltage and low power optimization of micro-heater and its on-chip drive circuitry for gas sensor array. *Sens. Actuators A Phys.* **100**(1), 94–101 (2002)
- A. Mozalev, R. Calavi, R.M. Vázquez, I. Gracia, C. Cane, X. Correig, X. Vilanova, F.G. Guirado, J.H. Iek, E. Llobet (2013), MEMS-microhotplate-based hydrogen gas sensor utilizing the nanostructured porous-anodic-alumina-supported WO₃ active layer, *Int. J. Hydrog. Energy* **38**, 8011–8021
- K. Oblova, I. Anastasia, S. Sergey, S. Nikolay, L. Alexandr, V. Alexey, S. Andrey, Fabrication of microhotplates based on laser micromachining of zirconium oxide. *Phys. Proc.* **72**, 485–489 (2015)
- A. Oprea, J. Courbat, N. Barsan, D. Briand, N.F. de Rooij, U. Weimar, Temperature, humidity and gas sensors integrated on plastic foil for low power applications. *Sens. Actuators B* **140**, 227–232 (2009)
- R. Phatthanakun, P. Deelda, W. Pummara, C. Sriphung, C. Pantong, N. Chomnawang, Design and fabrication of thin-film aluminum microheater and nickel temperature sensor, in *Proc. IEEE NEMS, Kyoto*, pp. 112–115 (2012)
- M. Prasad, Design, development and reliability testing of a low power bridge-type micromachined hotplate. *J. Microelectron. Reliab.* **55**(06), 937–944 (2015)
- M. Prasad, R.P. Yadav, V. Sahula, V.K. Khanna, FEM simulation of platinum-based microhotplate using different dielectric membranes for gas sensing applications. *J. Sens. Rev.* **32**(1), 59–65 (2012)
- C. Rossi, P.T. Boyer, D. Estbve, Realization and performance of thin SiO₂, SiN_x membrane for microheater applications. *Sens. Actuators A* **64**, 241–245 (1998)
- J. Sama, G. Domenech, R.R. Guillem, S. Albert, S. Michael, S. Barth, J. Santander, C. Calaza, I. Gracia (2017), Low temperature humidity sensor based on Ge nanowires selectively grown on suspended microhotplates, *Sens. Actuators B* **243**, 669–677 (p 9)
- F. Samaeifar, A. Afifi, H. Abdollahi, Simple fabrication and characterization of a platinum microhotplate based on suspended membrane structure. *Exp. Tech.* **40**, 755–763 (2016)
- N.N. Samotaev, B.I. Podlepetsky, A.A. Vasiliev, A.V. Pislakov, A.V. Sokolov, Metal-oxide gas sensor high-selective to ammonia. *Autom. Remote Control* **74**, 308–312 (2013)
- T. Seiyama, A. Kato, K. Fujushi, M. Nagatani, A new detector for gaseous components using semiconductive thin films. *Anal. Chem.* **34**(11), 1502–1503 (Oct. 1962)
- J.C. Shim, G.S. Chung, Fabrication and Characteristics of Pt/ZnO NO Sensor Integrated SiC Micro Heater, in *IEEE Sensors Conference*, pp. 350–353 (2010)

39. O. Sidek, M.Z. Ishak, M.A. Khalid, M.Z. Abu Bakar, M.A. Miskam, Effect of heater geometry on the high temperature distribution on a MEMS microhotplate. in *IEEE, 3rd Asia Symposium on Quality Electronic Design* (2011)
40. I. Simon, I.N. Barsan, M. Bauer, U. Weimar, Micromachined metal oxide gas sensors: opportunities to improve sensor performance. *Sens. Actuators B Chem.* **73**(1), 1–26 (2001)
41. R.M. Tiggelaar, Silicon-based microreactors for high-temperature heterogeneous partial oxidation reactions. Ph.D. dissertation. Univ. Twente, Enschede, 2004
42. G. Velmathi, N. Ramshanker, S. Mohan, Design, electro-thermal simulation and geometrical optimization of double spiral shaped microheater on a suspended membrane for gas sensing, in *Proc. 36th Annu. Conf. IEEE Ind. Electron. Soc.*, pp. 1258–1262 (2010)
43. D. Vincenzi, M.A. Butturi, V. Guidi, M.C. Carotta, G. Martinelli, V. Guarnieri, S. Brida, B. Margesin, F. Giacomozzi, M. Zen, G.U. Pignatelli, A.A. Vasiliev, A.V. Pisiakov, Development of a low-power thick-film gas sensor deposited by screen-printing technique onto a micromachined hotplate. *Sens. Actuators B Chem.* **77**, 95–99 (2001)
44. J. Wang, Z.A. Tang, A CMOS-compatible temperature sensor based on the gaseous thermal conduction dependent on temperature. *Sens. Actuators A* **176**, 72–77 (2012)
45. L. Xu, T. Li, X. Gao, Y. Wang, Development of a reliable micro-hotplate with low power consumption. *IEEE Sens. J.* **11**(4), 913–919 (2011)
46. Q. Zhou, A. Sussman, J. Chang, J. Dong, A. Zettl, W. Mickelson, Fast response integrated MEMS microheaters for ultra low power gas detection. *Sens. Actuators A Phys.* **223**, 67–75 (2015)